A novel Zn-based-MOF for efficient CO_2 adsorption and conversion under mild conditions

Jesús Tapiador [a], Pedro Leo [b], Antonio Rodríguez-Diéguez [c], Duane Choquesillo-Lazarte [d], Guillermo Calleja [a], Gisela Orcajo [a,*,1]

[a] *Department of Chemical, Energy and Mechanical Technology, ESCET, Rey Juan Carlos University, C/Tulipán s/n, 28933 Mostoles, Spain*
[b] *Department of Chemical and Environmental Technology, ESCET, Rey Juan Carlos University, C/Tulipán s/n, 28933 Mostoles, Spain*
[c] *Department of Inorganic Chemistry, University of Granada, Avda. Fuentenueva s/n, 18071 Granada, Spain*
[d] *Laboratorio de Estudios Cristalográficos, IACT, CSIC-Universidad de Granada, Avda. de las Palmeras 4, 18100 Armilla, Granada, Spain*

ARTICLE INFO

ABSTRACT

A novel Zn-based-MOF material, called Zn-URJC-8, containing two different organic linkers, 2-aminoterephtallic acid and 4,4-bipyridyl, has been synthetized and used for catalytic purposes for the first time. The structure of Zn-URJC-8 has been determined by single-crystal X-ray diffraction (XRD) showing -NH2 groups inward-facing of narrow pores, providing the material with excellent properties as CO_2 adsorbent. The good results obtained by means of carbon dioxide adsorption isotherms have demonstrated the high interaction between CO_2 and -NH2 groups with a Q_{st} value of 54 kJ/mol at low coverage. The Zn-URJC-8 material also display promising results as catalyst for CO_2 transformation in added value products. Almost complete conversion of epichlorohydrin and CO_2 in cycloaddition reaction has been achieved under mild conditions, and the influence of different radical groups coordinated to the epoxides has been evaluated on the reaction yield. The recyclability has been also tested and the structural integrity of the catalyst is maintained after several consecutive reaction cycles.

1. Introduction

Currently, the carbon dioxide emissions caused by human activity due to burning fossil fuels and biomass is generating several environmental impact in our planet like the well-known global warming [1,2], so it is tremendously compelling the need of reducing those CO_2 emissions. Different approaches are being conducted to efficient carbon capture and utilization (CCU) technologies [3]. C1 chemistry has emerged to transform molecules containing just a single carbon atom, like carbon dioxide, into value-added chemicals and clean fuels [4,5]. Carbon dioxide is an abundant, no-toxic, cheap and renewable source for C1 chemistry process. However, the thermodynamic stability of carbon dioxide molecule makes difficult its conversion, so many catalysts have been tested to overcome this limitation. However, there are many factors that make difficult their industrial application. For example, coordination complexes have been used as homogeneous catalysts with great yields, but these compounds have the intrinsic difficulty of being separated from the reaction media and then reused [6–11]. To solve this limitation, heterogeneous catalyst such as ionic liquid-supported solids, polymers, metal oxides, zeolites and porous organic frameworks have been explored, showing the advantages of easy separation and regeneration [12–19]. However, they have also shown short lifetime, poor recyclability, low selectivity and, in some of the cases, the need of a high temperature and CO_2 pressure to obtain high yields. Furthermore, many of products obtained from CO_2 molecule imply the use of H_2 such as reagent. Tao et al. indicated that only 0.1% of H_2 employed in these kind reactions is generated from renewables energies, so the remaining 99.9% H_2 is produced by fossil fuels which involves the emission of carbon dioxide to the atmosphere [20]. For these reasons, it is necessary to develop new high-efficient heterogeneous catalysts and processes that don't need direct H_2 inputs, avoiding the consumption of renewable electricity, that overcome all those constraints.

Metal-organic frameworks (MOFs) have emerged as promising high porous crystalline materials with remarkable properties, based on their unique structure constructed by organic linkers coordinated to metal ions or clusters. The great advantages of MOFs over other porous materials are their tunable structure-property features, hybrid composition,

defined and diverse crystal structure and high porosity [21–23]. These properties make them excellent materials in several applications as sensing, separation, gas storage, biomedicine, magnetics and heterogeneous catalysis [22, 24–27]. Due to their structural versatility, metal-organic frameworks can lodge Lewis acid and basic sites that improve their properties as catalyst in CO_2 conversion [28–31]. Lewis basic sites are functional groups with free electron pairs that can interact with carbon dioxide molecule increasing its reactivity, thus reducing the temperature and pressure required in CO_2 conversion reactions.

Five-membered cyclic carbonates are stable and no-toxic molecules that are used as solvents for battery electrolytes, resin materials and intermediates in pharmaceutical and plastic production processes [32, 33]. MOF materials have been tested as catalysts in the production of cyclic organic carbonates by means of CO_2 and epoxides cycloaddition reactions [34–36]. In these reactions, Lewis acid and basic sites play and important role to improve their conversion and selectivity, and besides high reaction temperatures and the use mono-substituted epoxides are usually required. To date, there is a limited number of MOFs reported with high yields and carbon dioxide conversions under free-solvent and mild conditions [37–39]. Gao et al. synthesized a new Cu-based-MOF, MMCF-2, which can achieve 95.4% of conversion in cycloaddition reaction of propylene oxide using nBu4NBr as co-catalyst [40]. Yan et al. reached total conversion in the reaction between propylene oxide and carbon dioxide at 100 °C, 1 bar and 16 h [41]. These works have shown that to attain high yields in cycloaddition reaction under mild conditions of temperature and pressure a co-catalyst in large amounts is needed or high temperatures. So, currently, it is highly desirable to develop new MOF materials capable to reach good yield values without co-catalyst and at moderate conditions [20].

In the search of commercially available organic molecules to act as ligands in the formation of novel MOF structures to have (i) high coordination number (structural stability), (ii) hydrophobicity and (iii) exhibiting Lewis's acid and/or basic sites desired for enhancing CO_2 conversion to cyclic carbonates, one approach is consisting in mixing organic molecules that provide those requirements. Some examples of this kind of mixed-ligand MOF catalysts used in these reactions are the following: Lan et al. synthesized a new Zn-based MOF using 3-amino-1,2,4-triazole and 3,5-pyridinedicarboxylic acid as ligands and achieved 96% yield in cycloaddition reaction of propylene oxide at 100 °C, 1.5 MPa for 5 h, using 0.1 g of TBAB as co-catalyst [42]. Wu et al. tested a MOF of Zn based on 1,3,5-benzenetricarboxylic acid and 2-methylimidazole getting a 97% yield in the cycloaddition of epichlorohydrin and CO_2 at 3.0 MPa, 100 °C and 6 h [43]. At the same time, Wu et al. employing methylamine and formic acid synthesized a novel Mn-based MOF, which obtained a 95% yield in the epichlorohydrin cycloaddition reaction under 1.5 MPa, 100 °C and 6 h [44].

The aim of this work is to develop a new efficient MOF catalyst to capture and transform CO_2 into high value products, in one step. Thus, a novel zinc-based MOF material having 2-aminoterephthalic acid and 4,4′-bipyridyl as organic linkers, containing Zn Lewis acid sites, the amino group that is a well-known electron-donor functionality (basic sites) that strongly interact with CO_2 molecules favoring its selective adsorption, and pyridine group to provide hydrophobicity to the structure that can reduce H_2O adsorption under industrial conditions, was synthetized and characterized. This material was then evaluated in CO_2 conversion to cyclic carbonates by reacting with epoxides under mild conditions, using epoxides with different functional groups. The recyclability of this catalyst was also tested.

2. Experimental section

2.1. Materials and measurements

All starting materials and solvents were purchased from Cymit Química S.L. and used without further purification.

2.2. Synthesis of Zn-URJC-8

0,1 mmol (0.029 g) of zinc nitrate hexahydrate, 0,1 mmol (0.018 g) of 2-aminoterephthallic acid and 0.2 mmol (0.031 g) of 4,4′-bipyridyl were mixed with 10 mL of DMF and 2 mL of H_2O in a 20 mL vial and sonicated for 15 min. Then, this yellow solution was heated at 90 °C for 72 h and cooled to room temperature. Yellow crystals were separated by filtration, washed three times with DMF and dried in air. Yield: 24% based on linker 2-aminoterephthallic acid. FT-IR: 3398 (w), 3325 (w), 3068 (w), 1660 (m), 1610 (s), 1571 (s), 1494 (s), 1421 (s), 1361 (s), 1257 (s), 1220 (m), 1145 (m), 1074 (s), 1049 (m), 1016 (m), 958 (m), 856 (m), 835 (w), 810 (s), 765 (s), 729 (w), 704 (w), 661 (w) and 642 (s) cm^{-1}.

2.3. Single crystal X-ray diffraction

Measured crystal was prepared under inert conditions immersed in perfluoropolyether as protecting oil for manipulation. Suitable crystal was mounted on MiTeGen Micromounts™, and these samples were used for data collection. Data for **Zn-URJC-8** was collected with a Bruker D8 Venture diffractometer. The data were processed with APEX3 suite [45]. The structure was solved by Intrinsic Phasing using the ShelXT program [46], which revealed the position of all non-hydrogen atoms. These atoms were refined on F^2 by a full-matrix least-squares procedure using anisotropic displacement parameters [47]. All hydrogen atoms were located in difference Fourier maps and included as fixed contributions riding on attached atoms with isotropic thermal displacement parameters 1.2 or 1.5 times those of the respective atom. The OLEX2 software was used as a graphical interface [48]. Crystallographic data for the reported structure have been deposited with the Cambridge Crystallographic Data Center as supplementary publication no. CCDC 2093467. Additional crystal data are shown in Table S1. Copies of the data can be obtained free of charge at http://www.ccdc.cam.ac.uk/products/csd/request.

2.4. Physicochemical characterization techniques

^{1}H NMR and ^{13}C NMR spectra were collected with a Varian Mercury Plus spectrometer at 400 MHz using trimethyl silane as an internal standard. FID files were processed using MestRe-C software version 4.9.9.6. The chemical shifts (δ) for ^{1}H spectra, given in ppm, are referenced to the residual proton signal of the deuterated chloroform. The chemical Shifts for ^{13}C spectra are referenced to the signal from the carbon of the deuterated solvent. Powder X-ray diffraction (PXRD) patterns were obtained in a Philips XPERT PRO (URJC, Móstoles, Spain) using CuKα (λ = 1.542 Å) radiation with a 0.01 step, 10 s of accumulation time between steps. In all the cases the sample were grounded to avoid the effects of preferred crystal orientation. High Temperature XRD in situ analysis was carried out under a dynamic air atmosphere of 1 mL/min with a heating ramp of 10 °C/min up to 350 °C. Fourier transform-infrared spectra (FT-IR) were recorded for powder samples in a Varian 3100 Excalibur Series spectrometer (URJC, Móstoles, Spain) with a resolution of 4 cm^{-1}. Simultaneous thermogravimetry and derivative thermogravimetry analyses (TGA/DTGA) were carried out under an air atmosphere with a Mettler-toledo DSC-TGA Star System device. Scanning electron microscopy (SEM) images and EDS analysis were obtained on a TM1000-Hitachi operated at 15 kV. Argon adsorption-desorption isotherms were measured at 87 K on an AutoSorb equipment (Quantachrome Instrument, URJC, Móstoles, Spain). The specific surface area was calculated by the Brunauer-Emmett-Teller (BET) equation [49].

2.5. CO_2 adsorption/desorption isotherms

Adsorption/desorption isotherms of pure CO_2 were obtained in a volumetric analyzer type VTI HPVA-100 Scientific Instrument. Approximately 200 mg of non-impregnated MOF materials were
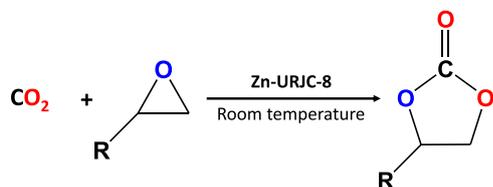
Scheme 1. Cycloaddition reaction of CO_2 and epoxides to carbonates.

previously evacuated in-situ under vacuum ($9 \cdot 10^{-3}$ bar) at 110 °C for 12 h, and then cooled down up to the analysis temperature in a thermostatic polyethyleneglycol bath. Isotherm equilibrium points were collected considering the following two equilibrium criteria: i) a pressure drop below 0.2 mbar in 3 min or ii) a maximum equilibrium time of 60 min. CO_2 adsorption equilibrium points at 25 and 45 °C were fitting with Sips equation (Sips, 1948). The Clausius-Clapeyron equation was used to determine the isosteric heat of adsorption from the slope of the best linear fit of ln(P) versus (1/T) at each CO_2 loading (additional details are included in SI).

## 2.6. *Catalytic studies of Zn-URJC-8 for the cycloaddition reaction of CO_2*

In a model experiment, 1 mmol of epoxide, 0.5–2.0 mol% (active metal sites to epoxide ratio) of degassed MOF catalyst and 0.05 mmol of tetrabutylammonium bromide (Bu_4NBr,) were added in a 100 mL stainless-steel autoclave (Scheme 1). The system was evacuated with CO_2 three times before being pressurized. Then, the reaction was carried out at room temperature under moderate stirring. Once the reaction time was completed, the residual carbon dioxide was slowly discharged and the catalyst was separated by centrifugation. To determine the reaction conversion and selectivity, the products were analyzed by 1 H NMR using $CDCl_3$ as solvent and 1, 2, 4, 5-tetrachloro-3-nitrobenzene as internal standard.

3. Results and discussion

3.1. *Structural description*

X-ray diffraction analysis performed on compound **Zn-URJC-8** shows that it crystallizes with the $\{[Zn_2(NH_2\text{-terepht})_2(4,4'\text{-bipy})_2]_{1.5}.2$
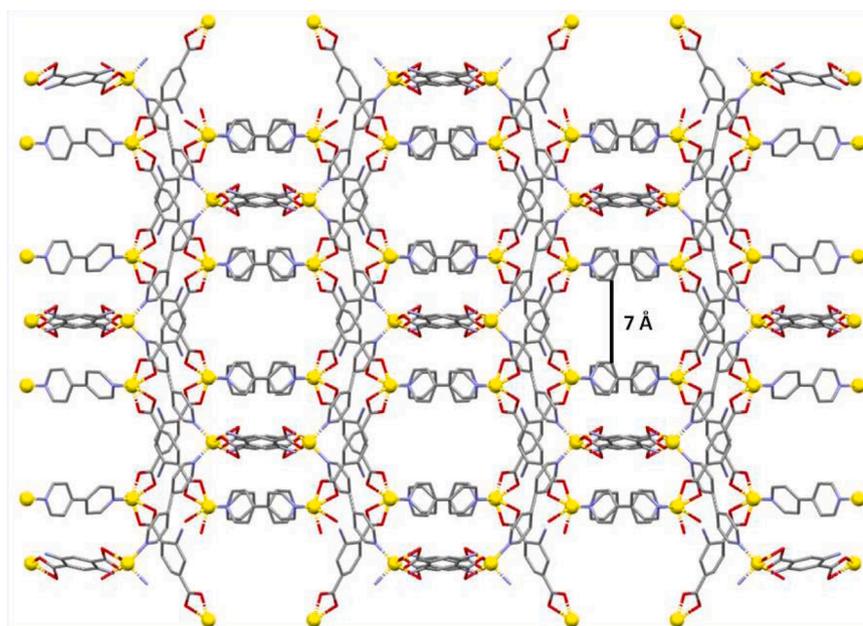
Fig. 1. View of the hexagonal grids of compounds Zn-URJC-8 showing the channels along the *c* axis. Only one of the three interpenetrated networks is displayed for the sake of clarity. color codes: yellow, zinc; red, oxygen; blue, nitrogen; gray, carbon. Hydrogen atoms have been omitted for clarity. (For interpretation of the references to colour in this figure legend, the reader is referred to the web version of this article.)
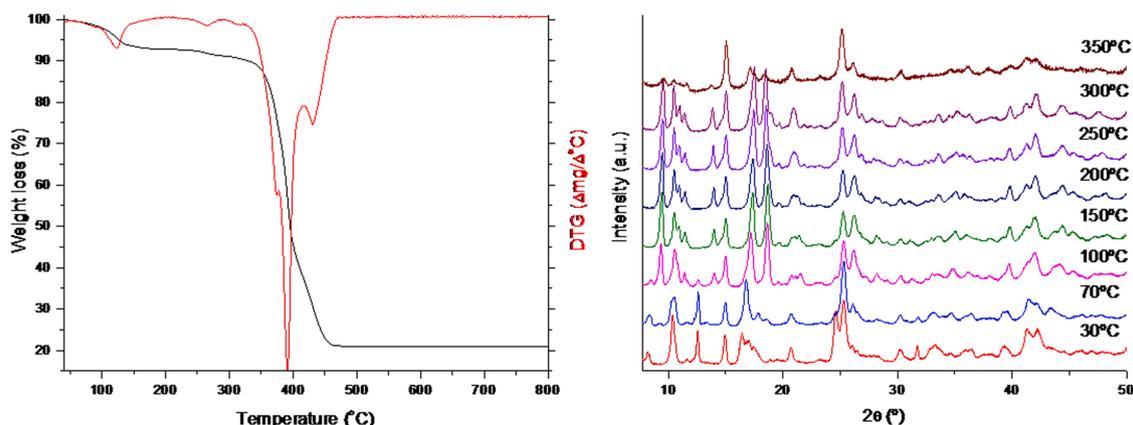

Fig. 2. TGA/DTG curves of Zn-URJC-8 (left). b) Temperature dependence PXRD patterns (right).
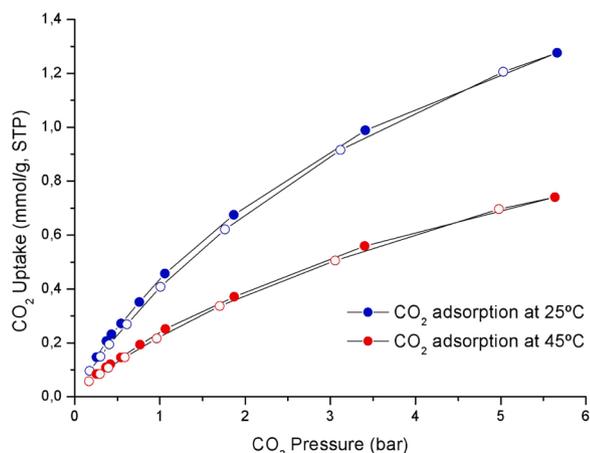
**Fig. 3.** CO$_2$ adsorption-desorption isotherms of Zn-URJC-8 at 25 and 45 °C.
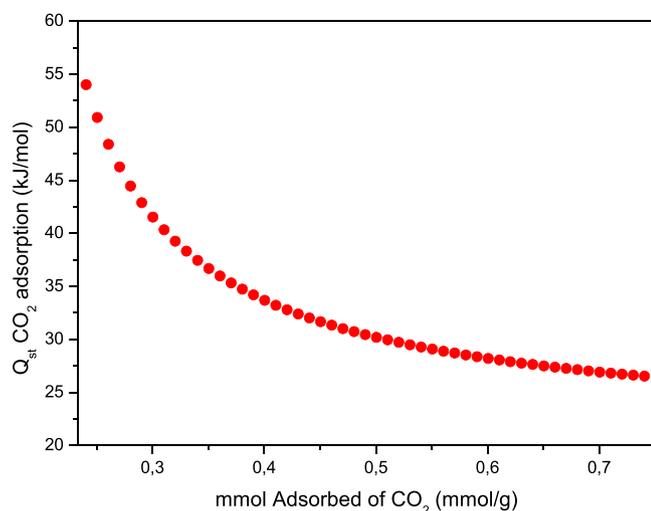
Fig. 4. Heat of CO$_2$ adsorption for Zn-URJC-8 estimated by Clausius-Clapeyron equation.

Table 1

CO$_2$ Q$_{st}$ value for different MOFs.

Material	Q$_{st}$ (kJ/mol)	Reference
Azo-DMOF-1	25	[51]
Zn4O-based-MOF	30	[52]
CoMOF-2	35	[53]
M-MOF-184 (M= Mg, Co, Ni and Zn	35, 33, 36 and 21	[54]
MIL-100(Cr)	62	[55]
bio-MOF-11	45	[56]
Amino-MIL-53(Al)	38	[57]
IRMOF-3	19	[58]
Co-MOF-74	37	[59]
HKUST-1	35	[60]
Zn-URJC-8	54	This work

Table 2

Zn-URJC-8 performance in CO$_2$ with epichlorohydrin cycloaddition reaction.[1]

Entry	% Catalyst	Pressure (bar)	Time (h)	ECH Conversion (%)	Yield[2] (%)
1	0.5	12	24	88	87
2	1.0	12	24	91	90
3	1.5	12	24	98	97
4	2.0	12	24	98	97
5	1.5	8	24	95	94
6	1.5	4	24	88	87
7	1.5	1	24	86	85
8	1.5	12	12	81	80
9	1.5	12	6	77	76
10	1.5	12	3	57	56

[1] Reaction conditions: ECH 1 mmol, 5 mol% co-catalyst, RT (25 °C).
[2] The yield of reaction was determined by ^{1}H-NMR analysis.

Table 3

Catalytic results in cycloaddition reaction with different Zn-based materials.[a]

Material	Conversion (%)
Zn(NO$_3$)$_2$·6H$_2$O	80
ZnBr$_2$	33
ZIF-8	76
Zn-MOF-74	98
ZnO	90
Zn-URJC-8	98

[a] epoxide: 1 mmol, 1.5% mol of catalyst, 5% mol co-catalyst, 12 bar of CO$_2$, RT (25 °C), 24 h. Selectivity > 98% in all cases.

almost identical very distorted octahedral coordination environments, in which The ZnN$_2$O$_4$ coordination sphere can be described by two nitrogen atoms pertaining to two 4,4′-bipyridyl ligand in cis positions while the other four positions are occupied by four carboxylate oxygen atoms pertaining to two 2-aminoterephthalic acid, in which all the carboxylate groups exhibit a μ-κ^2O,O′ coordination mode.

Zn−N and Zn-O distances are in the range of 2.07(2)–2.102(3) Å and 2.011(2)–2.475(3) Å, respectively. Zn^{II}···Zn^{II} distances through 2-aminoterephthalate and one 4,4′-bipyridyl ligands are 10.8 and 11.2 Å, respectively. The crystalline structure of this 3D MOF generates three types of channels along the *a*, *b* and *c* axes with amino groups oriented toward the center of the pores (Figs. S1.3 and S1.4). In Fig. 1, the clearest pore in the *c* axis has a largest dimension of 7 Å (before subtracting the Van der Waals radius of carbon atoms). Finally, Zn-URJC-8 shows strong hydrogen bonds (Fig. S1.5 left) involving hydrogen of amino groups and oxygen atoms pertaining to carboxylate (N-H...O bonds) with an average H-O distance of about 2.2 Å. The accessible volume of the structure is 36% measured with Mercury software, which reflects a bulky and dense scaffold (Fig. S1.5 right).

3.2. Catalyst characterization

After several synthesis attempts, high-quality yellow crystals for single crystal X-ray diffraction (XRD) were obtained, called Zn-URJC-8. Regarding powder X-ray diffraction (PXRD) technique, the as-prepared material revealed three main peaks at 9.35, 17.31 and 18.45° characteristic of this structure (Fig. S2.1.). The simulated powder XRD pattern of Zn-URJC-8 obtained by single XRD matched reasonably well with the experimental pattern, indicating both the high purity of the bulk sample and the successful single crystal resolution.

To study the thermal stability of novel material, TGA analysis in air atmosphere was carried out (Fig. 2a). Zn-URJC-8 was stable up to around 300 °C which corresponds to the starting of the organic linkers degradation with the subsequent collapse of the structure. Besides, the first weight loss of 6.5% observed between 40 and 150 °C was ascribed

(DMF)}$_n$ chemical formula in the monoclinic *C*2/*m* space group in the form of a 3D triply interpenetrated framework (Fig. 1) established by the coordination of zinc(II) atoms to the nitrogen and carboxylato oxygen atoms of the 4,4′-bipyridyl and 2-aminoterephthalic acid, respectively. The asymmetric unit is comprised by two crystallographically independent zinc atoms, each of them coordinated to one 2-aminoterephthalic acid and one 4,4′-bipyridyl ligand. Zn1 and Zn2 atoms show

Table 4

Zn-URJC-8 performance in the cycloaddition reaction of CO_2 and different epoxides.[a]

Entry	Epoxide	Product	Conversion (%)	Yield (%)
1			98	97
2			>99	98
3			93	92
4			90	89
5			59	58
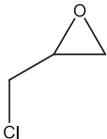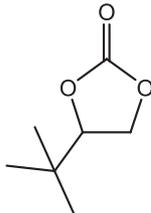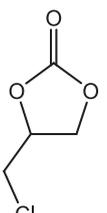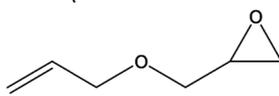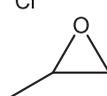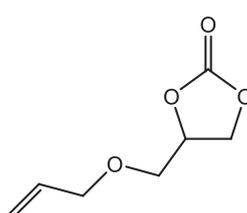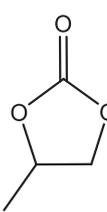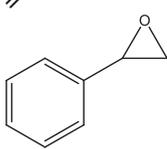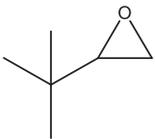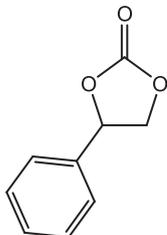
[a] epoxide: 1 mmol, 1.5% mol of catalyst, 5% mol co-catalyst, 12 bar of CO_2, RT (25 °C), 24 h.

to the loss of DMF guest molecules. The thermal stability was also studied by PXRD at different temperatures, which agrees on the remarkable structural integrity up to 300 °C (Fig. 2b). Thermogravimetric Analysis was also carried out after MOF activation under the conditions already mentioned in the experimental Section (3.5 mbar and 110 °C for 12 h). Observing the TGA profiles in Fig. S2.4 it is evident in that of Zn-URJC-8 after degas treatment (dash red line) that there is not the first weight loss related to solvent removal (centered at ca. 110 °C), so the only weight loss observed at c.a. 350 °C is that due to the organic ligand decomposition. The porosity of the zinc-based-MOF material was measured by argon adsorption/desorption isotherms at 87 K (Fig. S2.5), that corresponds to Type II isotherm of non-porous/macroporous materials, regarding the IUPAC classification [50]. This result agrees with the crystallographic information that evidenced a bulky and dense structure, and with TGA where a small weight loss of solvent removal was recorded. SEM images of Zn-URJC-8 material were recorded at different magnifications (Fig. S2.6), observing a homogeneous flower-like morphology in a crystal agglomeration with similar chemical composition along the bulk sample.

3.3. CO_2 adsorption studies

CO_2 adsorption isotherms have been carried out at 25 and 45 °C. The as-synthesized sample was degassed at 110 °C under vacuum for 12 h. The stability of original framework after degassing treatment was confirmed by PXRD analysis (Fig. S2.2.). CO_2 adsorption isotherms show a typical type-I behavior with an uptake of 1.28 and 0.74 mmol·g^{-1} at 25 and 45 °C, respectively (Fig. 3). These moderate values are possibly due to partial diffusion hindrances of CO_2 in the narrow pores (3–4 Å) of the structure due to a similar dimension between CO_2 molecule and the available pore diameter to host the guest gas. To know the interaction strength between CO_2 molecules and Zn-URJC-8 material, the heat of CO_2 adsorption was calculated by means of the Clausius-Clapeyron equation (Fig. 4). It was found as high as around 54 kJ/mol, which demonstrated a remarkable affinity to this molecule, that presumably can favor the activation of it in a subsequent reaction process with epoxides. This is a noticeable value compared to other well-known MOFs, as it is summarized in Table 1.
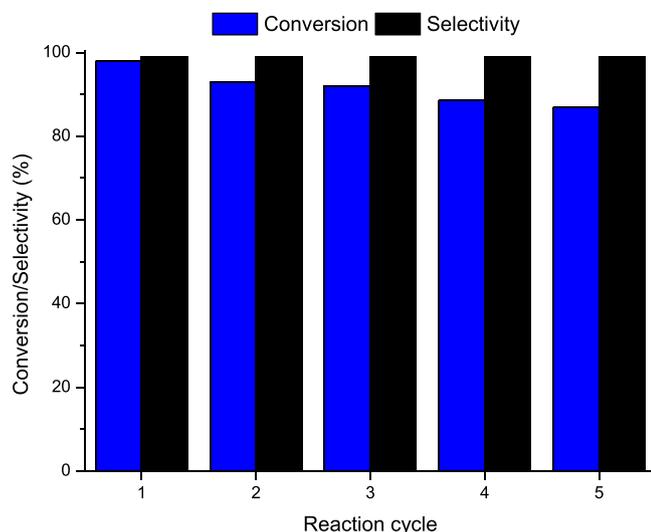
Fig. 5. Recyclability of Zn-URJC-8 in epichlorohydrin cycloaddition with CO_2.

3.4. Catalytic Cycloaddition reaction with CO_2 and different epoxides

The remarkable interaction of Zn-URJC-8 to CO_2 and the presence of Lewis acid and basic groups, that come from Zn^{2+} and NH_2 respectively, make this material an interesting candidate for further catalytic studies in the cycloaddition of mono and disubstituted epoxides with carbon dioxide. Firstly, the reaction was carried out with epichlorohydrin (ECH) at room temperature (25 °C) in presence of tetrabutylammonium bromide (TBAB) as co-catalyst. The influence of difference parameters in cycloaddition reaction was assessed, such as CO_2 pressure, amount of catalyst and time reaction (Table 2).

The influence of catalyst amount was evaluated in entries 1–4. There, it has been demonstrated that conversion and yield increase with the catalyst concentration from 0.5% to 1.5%, reaching almost complete conversion of epichlorohydrin; so 2.0% of catalysis in pointless to be used, even for the yield to the respective carbonate, which is similar than using 1.5%. When pressure decreases down to 1 bar (entries 3 and 5–7), both ECH conversion and yield slightly decrease, from 98% at 12 bar to 86% at 1 bar, because a higher pressure of carbon dioxide increases the solubility of the gas in the liquid phase, favoring this reaction. With respect to reaction time (entries 3 and 8–9), when it was fixed to 3 h the conversion was reduced to 57% compared to 98% when reaction lasted 24 h, which proved that reaction time is a critical factor. Besides, when the reaction was carried out without catalyst the conversion was found to be only 39%, indicating the essential role of Zn-URJC-8 catalyst in the performance of this reaction. No formation of secondary products was observed and the selectivity for cyclic carbonates was >99% in all cases. Hence, the optimal reaction conditions for the novel Zn-based-MOF were 1.5% mol of catalyst, 12 bar of CO_2 and a reaction time of 24 h.

The catalytic performance of other Zn-based materials has been tested in cycloaddition reaction of ECH and CO_2 and compared to the results obtained for Zn-URJC-8 (Table 3). In general speaking, the highest conversion is shown for the novel Zn-URJC-8 catalyst among different homogeneous and heterogeneous Zn catalysts. Particularly, for homogeneous $Zn(NO_3)_2 \cdot 6H_2O$ a epoxide conversion attained was 80% with its intrinsic catalyst recovery issues. The other salt ($ZnBr_2$) was not soluble in the media and only 33% of conversion was detected. Among heterogeneous catalyst, the best performance was shown for Zn-MOF-74, with a similar epoxide conversion found for our novel MOF, possibly due to the presence of -OH groups in its structure which make similar electron-donor effect than $-NH_2$ groups in Zn-URJC-8, that can increase the reactivity of carbon dioxide molecule. Nevertheless, the XRD analysis of MOFs after reaction (Figs. S4.17, S4.18) showed a partial crystallinity reduction for Zn-MOF-74 phase, since the broaden of

all the diffraction peaks, meanwhile the minimal degradation of the new Zn-URJC-8 after five reaction cycles (Fig. S6.1).

3.5. Catalytic activity for various epoxides with different radical groups

Due to the remarkable results in cycloaddition of epichlorohydrin, other epoxides were also tested under the optimal reaction conditions found for epichlorohydrin. Various epoxides with different functional groups and molecule size were selected, such us propylene oxide (entry 2) 3,3-dimethyl-1,2-epoxybutane (entry 3), allyl 2,3-epoxypropyl ether (entry 4) and styrene oxide (entry 5). The results obtained are summarized in Table 4.

As observed, the reaction yield was decreasing progressively as functional groups were bulkier (entries 2–4). This behavior can be attributed to the larger size of epoxide molecules compared to ECH, except for the case of propylene oxide for which maximum conversion and yield were obtained, owing to $-CH_3$ group size, which is smaller than $-CH_2Cl$ radical. When styrene oxide was used (entry 5), the yield of reaction decreased to 58%, compared to 97% for ECH. This moderate yield may be due to higher steric hindrance generated by the aromatic ring volume and its rigidity. When allyl 2,3-epoxypropyl ether was used, reaction conversion was found to be 90%, as a result of the longer chain of five members.

3.6. Recyclability of Zn-URJC-8

To test the recyclability of Zn-URJC-8 material, the same portion of MOF was reused in successive catalytic cycles for epichlorohydrin cycloaddition with CO_2 (12 bar of CO_2, 5% mol co-catalyst, room temperature and 24 h of reaction time), separating from liquid phase by centrifugation, washing with methanol and activating at 110 °C each time before next cycle. The conversion reaction was slightly decreasing with the number of cycles from 98% in the first cycle to 87% in the fifth one (Fig. 5). The crystal integrity of Zn-URJC-8 was checked by PXRD analysis after the five reaction cycles, confirming the permanence of its original crystalline phase (Fig. S6.1.); however, a slight loss of crystallinity was detected as well as the appearance of additional small peaks at 15.01 and 25.42° (Fig. S6.1.) of an unknown phase.

4. Conclusions

A novel metal-organic framework, Zn-URJC-8, using $Zn(NO_3)_2$ and two organic linkers: 2-aminoterephthalic acid and 4,4′-bipyridyl, has been synthetized and used for catalytic purposes for the first time. This MOF has been successfully synthesized and characterized by different physico-chemical techniques. Its structure was determined by single crystal X-ray diffraction, showing a 3D structure with channels along the crystallographic *a* and *c*-axes. This material present Lewis acid and basic sites, that come from Zn^{2+} and $-NH_2$ groups, respectively, having good properties as adsorbent and catalyst in CO_2 capture and conversion in one step. Zn-URJC-8 showed a CO_2 uptake of 28,27 $cm^3 \ g^{-1}$ at 25 °C and a Q_{st} value of 54 kJ/mol, higher than values obtained by other well-known reported MOFs used for CO_2 retention, which confirms its great affinity for CO_2. However, the moderate values of CO2 adsorption capacity are possibly due to partial diffusion hindrances of CO_2 in the narrow pores (3–4 Å) of the structure due to a similar dimension between CO_2 molecule and the available pore diameter to host the gas. Zn-URJC-8 as catalyst in the cycloaddition reaction of different epoxides with CO_2, showed almost complete conversion of epoxides under mild conditions. There is an influence of radical groups in the epoxide molecules on cycloaddition reactions, evidencing steric hindrances and a decrease in the reaction yield when bulkier epoxides are used. Finally, Zn-URJC-8 was tested in successive catalytic cycles, observing high stability in terms of catalytic activity and crystalline structure. These results make this novel material a promising catalyst for CO_2 conversion, providing new attractive options to face the global warming problem.

CRediT authorship contribution statement

Jesús Tapiador: Investigation, Writing – original draft. **Pedro Leo:** Conceptualization, Methodology. **Antonio Rodríguez-Diéguez:** Investigation. **Duane Choquesillo-Lazarte:** Investigation. **Guillermo Calleja:** Supervision, Funding acquisition. **Gisela Orcajo:** Supervision, Writing – review & editing, Conceptualization, Methodology.

Declaration of Competing Interest

The authors declare that they have no known competing financial interests or personal relationships that could have appeared to influence the work reported in this paper.

Appendix A. Supporting information

Supplementary data associated with this article can be found in the online version at doi:10.1016/j.cattod.2021.11.025.

References

[1] A. Schoedel, Z. Ji, O.M. Yaghi, Nat. Energy 1 (2016) 16034–16046.
[2] K. sumida, D.L. Rogow, J.A. Mason, T.M. McDonald, E.D. Bloch, Z.R. Herm, T. H. Bae, J.R. Long, Chem. Rev. 112 (2012) 724–781.
[3] C.A. Trickett, A. Helal, B.A. Maythalony, Z.H. Yamani, K.E. Cordova, O.M. Yaghi, Nat. Rev. Mater. 2 (2017) 17045.
[4] C. Mesters, Annu Rev, Chem. Biomol. 7 (2016) 223–238.
[5] C.B. Rberts, N.O. Elbashier, Fuel Process. Technol. 83 (2003) 1–9.
[6] D.J. Darensbourg, M.W. Holtcamp, Coord. Chem. Rev, 153, 1996, pp. 155–174.
[7] J.A. Widegren, R.G. Finker, J. Mol. Catal. A Chem. 198 (2003) 317–341.
[8] C. Copÿret, M. Chabanas, R.P. Saint-Arroman, J.M. Basset, Angew. Chem. Int. Ed. 42 (2003) 156–181.
[9] V.B. Saptal, B.M. Bhanage, ChemSusChem 9 (2016) 1980–1985.
[10] Y.D. Li, D.X. Cui, J.C. Zhu, P. Huang, Z. Tian, Y.Y. Jia, Wang PA, Green Chem. 21 (2019) 5231–5237.
[11] C. Martin, G. Fiorani, ACS Catal. 5 (2015) 1353–1370.
[12] J. Dong, P. Cui, P.F. Shi, P. Cheng, B. Zhao, J. Am, Chem. Soc. 137 (2015) 15988–15991.
[13] K. Kossev, N. Koseva, K. Troev, J. Mol. Catal. A Chem. 194 (2003) 29–37.
[14] Y. Xie, T.T. Wang, X.H. Liu, K. Zou, W.Q. Deng, Nat. Commun. 4 (2013) 1960.
[15] G.K. Cui, J.J. Wang, S.J. Zhang, Chem. Soc. Rev. 45 (2016) 4307–4339.
[16] Q. Sun, Y.Y. Jin, B. Aguila, X.J. Meng, S.Q. Ma, F.S. Xiao, ChemSusChem 10 (2017) 1160–1165.
[17] P. Schwach, X. Pan, X. Bao, Chem. Rev. 117 (2017) 8497–8520.
[18] M.H. Mahyuddin, A. Staykow, Y. Shiota, K. Yoshizawa, A.C.S. Catal 6 (2016) 8321–8331.
[19] G.J. Zhang, A.T. Su, Y.N. Du, J.W. Qu, Y. Xu, J. Colloid Interface Sci. 433 (2014) 149–155.
[20] L. Tao, T.S. Choksi, W. Liu, J. Pérez-Ramírez, ChemSusChem 13 (23) (2020) 6066–6089.
[21] H.C. Zhou, S. Kitagawa, Chem. Soc. Rev. 43 (2014) 5415–5418.
[22] H.C. Zhou, J.R. Long, O.M. Yaghi, Chem. Rev. 112 (2012) 673–674.
[23] N. Li, R. Feng, J. Zhu, Z. Chang, X.H. Bu, Coord, Chem. Rev. 375 (2018) 558–586.
[24] A. Kirchon, L. Feng, H.F. Drake, E.A. Joseph, H.C. Zhou, Chem. Soc. Rev. 47 (2018) 8611–8638.
[25] H. Wang, Q.L. Zhu, R. Zou, Q. Xu, Chem 2 (2017) 52–80.
[26] J. Liu, C. Wöll, Chem. Soc. Rev. 46 (2017) 5730–5770.
[27] M. Yoon, R. Srirambalaji, K. Kim, Chem. Rev. 112 (2012) 1196–1231.
[28] M. North, R. Pasquale, Angew. Chem. Int. Ed. 48 (2009) 2946–2948.
[29] T. Lescouet, C. Chizallet, D. Farrusseng, ChemCatChem 4 (2012) 1725–1728.
[30] M. Cabrero-Antonino, S. Remiro-Buenamañana, M. Souto, A.A. García-Valdivia, D. Choquesillo-Lazarte, S. Navalón, A. Rodríguez-Diéguez, G. Mínguez-Espallargas, H. García, Chem. Commun. 55 (2019) 10932.
[31] J. Liang, Y.-B. Huang, R. Cao, Coord. Chem. Rev. 378 (2019) 32–65.
[32] J. Bayardon, J. Holz, B. Schaffner, V. Andrushko, S. Verevkin, A. Preetz, A. Borner, Angew. Chem. Int. Ed. 46 (2007) 5971–5974.
[33] A.A. Olajire, Renewable Sustainable, Energy Rev. 92 (2018) 570–607.
[34] J.W. Maina, C. Pozo-Gonzalo, L. Kong, J. Schütz, M. Hill, L.F. Dumée, Mater. Horiz. 4 (2017) 345–361.
[35] M. Ding, R.W. Flaig, H.-L. Jiang, O.M. Yagui, Chem. Soc. Rev. 48 (2019) 2783–2828.
[36] H. He, J.A. Perman, G. Zhu, S. Ma, Small 12 (2016) 6309–6324.
[37] W.Y. Gao, Y. Chen, Y. Niu, K. Williams, L. Cash, P.J. Perez, L. Wojtas, J. Cai, Y. S. Chen, S. Ma, Angew. Chem. Int. Ed. 53 (2014) 2615–2619.
[38] O.V. Zalomaeva, A.M. Chibiryaev, K.A. Kovalenko, O.A. Kholdeeva, B. S. Balzhinimaev, V.P. Fedin, J. Catal 298 (2013) 179–185.
[39] P.J. Kitson, R.J. Marshall, D. Long, R.S. Forgan, L. Cronin, Angew. Chem. Int. Ed. 53 (2014) 1–7.
[40] W.-Y. Gao, Y. Chen, Y. Niu, K. Williams, L. Cash, P.J. Perez, L. Wojtas, J. Cai, Y.-S. Chen, S. Ma, Angew. Chem. Int. Ed. 53 (2014) 2615–2619.
[41] Y.-H. Han, Z.-Y. Zhou, C.-B. Tiana, S.-W. Du, Green Chem. 18 (2016) 4086–4091.
[42] J. Lan, Y. Qu, X. Zhang, H. Ma, P. Xu, J. Sun, J. CO2 Util. 35 (2020) 216–224.
[43] Y. Wu, X. Song, J. Zhang, S. Xu, N. Xu, H. Yang, Y. Miao, L. Gao, J. Zhang, G. Xiao, Chem. Eng. Res. Des. 140 (2018) 273–282.
[44] Y. Wu, X. Song, J. Zhang, S. Xu, L. Gao, J. Zhang, G. Xiao, Chem. Eng. Sci. 201 (2019) 288–297.
[45] Bruker, Bruker AXS Inc. V2019.1, Madison, Wisconsin, USA, 2019.
[46] G.M. Sheldrick, SHELXT - Integrated space-group and crystal-structure determination, Acta Crystallogr. Sec. A 71 (2015) 3–8, https://doi.org/10.1107/S2053273314026370.
[47] G.M. Sheldrick, Crystalstructure refinement with SHELXL, Acta Crystallogr. Sect. C 71 (2015) 3–8, https://doi.org/10.1107/S2053229614024218.
[48] O. Dolomanov, L.J. Bourhis, R. Gildea, J.A. Howard, H. Puschmann, OLEX2: a complete structure solution, refinement and analysis program, J. Appl. Crystallogr. 42 (2009) 339–341, https://doi.org/10.1107/S0021889808042726.
[49] S. Brunauer, P. Emmett, E. Teller, Adsorption of gases in multimolecular layers, J. Am. Chem. Soc. 60 (1938) 309–319.
[50] M. Thommes, K. Kaneko, A.V. Neimark, J.P. Olivier, F. Rodriguez-Reinoso, J. Rouquerol, K.S.W. Sing, Pure Appl. Chem. 87 (2015) 1051–1069.
[51] N. Prasetya, B.P. Ladewig, ACS Appl. Mater. Interfaces 10 (40) (2018) 34291–34301.
[52] H.F. Zhou, B. Liu, L. Hou, W.Y. Zhang, Y.Y. Wang, Chem. Commun. 54 (5) (2018) 456–459.
[53] P. Patel, B. Parmar, R.S. Pillai, A. Ansari, N.H. Khan, E. Suresh, Appl. Catal. A Gen. 590 (2020), 117375.
[54] Y.B.N. Tran, P.T.K. Nguyen, Q.T. Luong, K.D. Nguyen, Inorg. Chem. 59 (2020) 16747–16759.
[55] P. Llewellyn, S. Bourrelly, C. Serre, A. Vimont, M. Daturi, L. Hamon, G. Weireld, J. Chang, D. Hong, Y. Hwang, S. Jhung, G.F. Rey, Langmuir 24 (14) (2008) 7245–7250.
[56] J. An, S. Geib, N. Rosi, Am. Chem. Soc. 132 (2010) 38–39.
[57] S. Couck, J. Denayer, G. Baron, T. Rémy, J. Gascon, F. Kapteijn, J. Am. Chem. Soc. 131 (2009) 6326–6327.
[58] D. Farrusseng, C. Daniel, C. Gaudillère, U. Ravon, Y. Schuurman, C. Mirodatos, Langmuir 25 (2009) 7383–7388.
[59] S. Caskey, A. Wong, A. Matzger, J. Am. Chem. Soc. 130 (2008) 10870–10871.
[60] Q. Min, D. Shen, M. Bülow, M. Ling, S. Deng, F. Fitch, Microporous Mesoporous Mater. 55 (2002) 217–230.